Modeling financial sector joint tail risk in the euro area*

André Lucas,[(a)] *Bernd Schwaab,*[(b)] *Xin Zhang*[(c)]

[(a)] VU University Amsterdam and Tinbergen Institute

[(b)] European Central Bank, Financial Research Division

[(c)] Sveriges Riksbank, Research Division

First version: May 2013

This version: October 2014

*Author information: André Lucas, VU University Amsterdam, De Boelelaan 1105, 1081 HV Amsterdam, The Netherlands, Email: a.lucas@vu.nl. Bernd Schwaab, European Central Bank, Kaiserstrasse 29, 60311 Frankfurt, Germany, Email: bernd.schwaab@ecb.int. Xin Zhang, Research Division, Sveriges Riksbank, SE 103 37 Stockholm, Sweden, Email: xin.zhang@riksbank.se. We thank conference participants at the Banque de France & SoFiE conference on "Systemic risk and financial regulation", the Cleveland Fed & Office for Financial Research conference on "Financial stability analysis", the European Central Bank, the FEBS 2013 conference on "Financial regulation and systemic risk", LMU Munich, the 2014 SoFiE conference in Cambridge, the 2014 workshop on "The mathematics and economics of systemic risk" at UBC Vancouver, and the Tinbergen Institute Amsterdam. André Lucas thanks the Dutch Science Foundation (NWO, grant VICI453-09-005) and the European Union Seventh Framework Programme (FP7-SSH/2007-2013, grant agreement 320270 - SYRTO) for financial support. The views expressed in this paper are those of the authors and they do not necessarily reflect the views or policies of the European Central Bank or the Sveriges Riksbank.

Modeling financial sector joint tail risk in the euro area

Abstract

We develop a novel high-dimensional non-Gaussian modeling framework to infer conditional and joint risk measures for many financial sector firms. The model is based on a dynamic Generalized Hyperbolic Skewed-t block-equicorrelation copula with time-varying volatility and dependence parameters that naturally accommodates asymmetries, heavy tails, as well as non-linear and time-varying default dependence. We demonstrate how to apply a conditional law of large numbers in this setting to define risk measures that can be evaluated quickly and reliably. We apply the modeling framework to assess the joint risk from multiple financial firm defaults in the euro area during the 2008-2012 financial and sovereign debt crisis. We document unprecedented tail risks during 2011-12, as well as their steep decline after subsequent policy actions.

Keywords: systemic risk; dynamic equicorrelation; generalized hyperbolic distribution; law of large numbers; large portfolio approximation.

JEL classification: G21, C32.

1 Introduction

In this paper we develop a novel high-dimensional non-Gaussian modeling framework to infer conditional and joint risk measures for many financial sector firms. The model is based on a dynamic Generalized Hyperbolic Skewed-t copula with time-varying volatility and dependence parameters. Such a framework naturally accommodates asymmetries, heavy tails, as well as non-linear and time-varying default dependence. To balance the need of parsimony as well as flexibility in a high-dimensional cross-section, we endow the dynamic model with a score driven block-equicorrelation structure. We further demonstrate that a conditional law of large numbers applies in our setting which allows us to define risk measures that can be evaluated easily and reliably within seconds. We apply the modeling framework to assess the joint risk from multiple financial firm defaults in the euro area during the financial and sovereign debt crisis. We document unprecedented tail risks during 2011-12, as well as a sharp decline in joint (but not conditional) tail risk probabilities after a sequence of announcements by the European Central Bank (ECB) that introduced its Outright Monetary Transactions (OMT) program.[1]

Since the onset of the financial crisis in 2007, financial stability monitoring has become a key priority for many central banks, in addition to their respective monetary policy mandates, see for example Acharya, Engle, and Richardson (2012), and Adrian, Covitz, and Liang (2013). Central banks and related authorities have received prudential responsibilities that involve the analysis of financial risks to and from a large system of financial intermediaries. The cross sectional dimensions of these systems are typically high, even if attention is restricted to only large and systemically important institutions. Our modeling framework is directly relevant for such monitoring tasks. In addition, our framework is interesting for financial institutions and clearing houses that are required to actively set risk limits and maintain economic capital buffers to withstand bad risk outcomes due to exposures to a large number of credit risky counterparties. Finally, with the benefit of hindsight, an evaluation of the time variation in conditional and joint risks allows us to assess the impact of non-standard policy measures undertaken by central banks (or other actors) on the risk of a simultaneous and widespread failure of financial intermediaries.

Using our framework, we repeatedly now-cast market participants' current perceptions about financial system risks as impounded into asset prices, such as equities. This also involves the use of risk measures derived from such prices, such as expected default frequencies (EDF) typically used in the industry. Our starting point for modeling time-varying joint and conditional risks is a dynamic copula framework, as for example also considered by Avesani, Pascual, and Li (2006), Segoviano and Goodhart (2009), Oh and Patton (2013), Christoffersen, Jacobs, Jin, and Langlois (2013), and Lucas, Schwaab, and Zhang (2014). In each case, a collection of firms is seen as a portfolio of obligors whose multivariate dependence

[1]See ECB (2012b) and Coeuré (2013). The OMT is a non-standard monetary policy measure within which the ECB could, under certain conditions, make purchases in secondary markets of bonds issued by euro area member states.

structure is inferred from equity (or CDS) data. For example, Avesani, Pascual, and Li (2006) assess defaults in a Gaussian factor model framework. Their determination of joint default probabilities is in part based on the notion of an nth-to-default CDS basket, which can be set up and priced as suggested in Hull and White (2004). Alternatively, Segoviano and Goodhart (2009) propose a non-parametric copula approach. Here, the multivariate density is recovered by minimizing the distance between the so-called banking system's multivariate density and a parametric prior density subject to tail constraints that reflect individual default probabilities. We regard each of these two earlier approaches as polar cases, and attempt to strike a middle ground. The framework in our current paper retains the ability to describe the salient equity data features in terms of skewness, fat tails, and time-varying correlations (which the static Gaussian copula model fails to do), and in addition retains the ability to fit a cross-sectional dimension larger than a few firms (which the non-parametric approach fails to do due to computational problems). Relatedly, Oh and Patton (2013) and Christoffersen et al. (2013) study non-Gaussian and high-dimensional risk dependence in the U.S. non-financial sector using the dynamic skewed Student's t density of Hansen (1994), rather than the Generalized Hyperbolic Skewed-t of the current paper.

Our study contributes to several directions of current research. First, we effectively apply 'market risk' methods to solve a 'credit risk' problem. As a result, we connect a growing literature on non-Gaussian volatility and dependence models with another literature on credit risk and portfolio loss asymptotics. Time-varying parameter models for volatility and dependence have been considered, for example, by Engle (2002), Demarta and McNeil (2005), Creal et al. (2011), Zhang et al. (2011), and Engle and Kelly (2012). At the same time, credit risk models and portfolio tail risk measures have been studied, for example, by Vasicek (1987), Lucas et al. (2001, 2003), Gordy (2000, 2003), Koopman, Lucas and Schwaab (2011, 2012), and Giesecke et al. (2014). We argue that our combined framework yields the best of these two worlds: portfolio credit risk measures (say, one year ahead) that are available at a market risk frequency (such as daily or weekly) for real time portfolio risk measurement. A third strand of literature investigates joint and conditional default dependence from a financial stability perspective, see, for example, Hartmann, Straetmans, and de Vries (2007), Acharya, Engle, and Richardson (2012), Malz (2012), Suh (2012), Black, Correa, Huang, and Zhou (2012), and Lucas et al. (2014). Fourth, to balance the need for parsimony and flexibility, we consider a variant of a block dynamic equicorrelation (DECO) structure for the covariance matrix as in Engle and Kelly (2012). The version developed in this paper of the block equicorrelation model still allows us to draw upon machinery developed in the credit portfolio tail risk literature mentioned earlier. Finally, to introduce time-variation into our econometric model specification we endow our model with observation-driven dynamics based on the score of the conditional predictive log-density. Score-driven time-varying parameter models are an active area of research, see for example Creal, Koopman, and Lucas (2011), Creal, Koopman, and Lucas (2013), Harvey (2013), Oh and Patton (2013), Creal, Schwaab, Koopman, and Lucas (2014), Harvey and Luati (2014), Andres (2014), and more.[2] For an information theoretical motivation for the use of score driven models, see Blasques, Koopman, and Lucas (2014b).

We apply our general framework by analyzing financial sector joint and conditional default risks of $N = 10$ and $N = 73$ financial sector firms located in the euro area, based on weekly data from January 1999 to September 2013. Using a limited dimension of $N = 10$ firms, we verify that our dynamic correlations based on the (block) DECO assumption closely track the average correlations from a full correlation matrix model analysis. In addition, we verify that our semi-analytical approximations to compute joint and conditional tail risk measures already work well even if the cross-sectional dimension is as low as 10 firms. In our final high-dimensional ($N = 73$) application, we document unprecedented joint tail risks for a set of large euro area financial sector firms during the financial and euro area sovereign debt crises. We also document a clear peak of financial sector joint default risk in the summer of 2012. Based on time variation in our joint risk measure we argue that three events — a speech by the ECB president in London on 26 July 2012, the announcement of the Outright Monetary Transactions (OMT) program on 2 August 2012, and the disclosure of the OMT details on 6 September 2012 — collectively ended the most acute phase of extreme financial sector joint tail risks in the euro area. Second, we document that conditional tail probabil-

[2] We refer to `http://www.gasmodel.com` for an extensive enumeration of recent work in this area.

ities did not decline as much, indicating that risk spillovers may have remained a concern. Taken together, these findings suggests that the OMT was perceived by market participants less in terms of a 'firewall' measure that mitigates risk spillovers, but rather in terms of a mechanism that impacts marginal risks but not necessarily the connectedness of financial sector firms. Finally, we argue that the design and implementation of non-standard monetary policy measures and financial stability (tail) outcomes are strongly related. This finding suggests substantial scope for the coordination of monetary, macro-prudential, and bank supervision policies. This is relevant as both monetary policy as well as banking supervision will be carried out jointly by the ECB as of November 2014.

The remainder of the paper is set up as follows. Section 2 introduces our statistical framework, the dynamic Generalized Hyperbolic Skewer-t Block DECO model, and discusses parameter estimation. Section 3 demonstrates how a conditional law of large numbers can be applied to portfolio risk measures in a GHST factor copula setting, which enables us to compute such measures reliably and quickly. Section 4 applies the modeling framework to the euro area financial sector during the financial and sovereign debt crisis. Section 5 concludes. The Appendix presents proofs and additional technical details.

2 Statistical model

2.1 The dynamic Generalized Hyperbolic Skewed t copula model

Following Lucas et al. (2014), we consider a copula model based on the Generalized Hyperbolic Skewed t (GHST) distribution. Let

$$y_{it} = (\varsigma_t - \mu_\varsigma)\gamma_i + \sqrt{\varsigma_t}\,\tilde{\Sigma}_t^{1/2}\epsilon_t, \qquad i = 1, \ldots, N, \tag{1}$$

where $\epsilon_t \in \mathbb{R}^N$ is a vector of standard normally distributed risk factors, $\tilde{\Sigma}_t \in \mathbb{R}^{N\times N}$ is the GHST copula scale matrix, $\gamma \in \mathbb{R}^N$ is a vector controlling the skewness of the copula, and $\varsigma_t \in \mathbb{R}^+$ is an inverse-Gamma distributed common risk factor that affects all firms simultaneously, $\varsigma_t \sim \mathrm{IG}(\frac{\nu}{2}, \frac{\nu}{2})$. The two random variables ς_t and ϵ_t are independent, and we set $\mu_\varsigma = \mathrm{E}[\varsigma_t] = \nu/(\nu-2)$, such that y_{it} has zero mean if $\nu > 2$. Matrix $\tilde{\Sigma}_t^{1/2}$ is a matrix square root of $\tilde{\Sigma}_t$.

A firm defaults if y_{it} falls below its default threshold y_{it}^*. The cross sectional dependence in defaults captured by equation (1) thus stems from two sources: common exposures to the normally distributed risk factors ϵ_t as captured by the time-varying matrix $\tilde{\Sigma}_t$; and an additional common exposure to the scalar risk factor ς_t. The former captures connectedness through correlations, while the latter captures such effects through the tail-dependence of the copula. To see this, note that if ς_t is non-random, the first term in (1) drops out of the equation and there is zero tail dependence. Conversely, if ς_t is large, all asset values are affected at the same time, making joint defaults of two or more firms more likely.

Earlier applications of the GHST distribution to financial and economic data include, for example, Mencía and Sentana (2005), Hu (2005), Aas and Haff (2006), and Oh and Patton (2013). Alternative skewed t distributions have been proposed as well, such as Branco and Dey (2001), Gupta (2003), Azzalini and Capitanio (2003), and Bauwens and Laurent (2005); see also the overview of Aas and Haff (2006). An advantage of the GHST distribution vis-à-vis these alternatives is that the GHST assumption relates more closely to the continuous-time finance literature under skewness and fat tails; see for example Bibby and Sørensen (2001).

Define the default probability for firm i at time t as p_{it}, such that

$$p_{it} = \Pr\left[y_{it} < y_{it}^*\right] = \mathrm{F}_{it}(y_{it}^*) \Leftrightarrow y_{it}^* = \mathrm{F}_{it}^{-1}(p_{it}), \tag{2}$$

where F_{it} is the univariate GHST cumulative distribution function (cdf) of y_{it}. In our application, we assume that we observe p_{it} as the expected default frequency of firm i reported at time t by Moody's. Instead of focusing on the individual default probabilities p_{it}, our focus is instead on the time-varying *joint* probabilities, such as $\Pr\left[y_{it} < y_{it}^*, y_{jt} < y_{jt}^*\right]$, or on the conditional probabilities $\Pr\left[y_{it} < y_{it}^* | y_{jt} < y_{jt}^*\right]$, for firms $i \neq j$. Below, we first develop a dynamic version of the GHST copula model. We then consider a dynamic (block)-equicorrelation version of the model in the spirit of Engle and Kelly (2012), which turns out to be particularly useful to study joint and conditional default probabilities in a parsimonious way for large dimensional systems.

2.2 The dynamic GHST model

To describe the dynamics of the scale parameter $\tilde{\Sigma}_t$ in the GHST model (1), we use the generalized autoregressive score (GAS) dynamics as proposed in Creal et al. (2011, Creal et al. (2013); see also Harvey (2013). These dynamics easily adapt to the skewed and fat-tailed nature of the GHST density and improve the stability of dynamic volatility and correlation estimates; see Blasques et al. (2014b). Our version of the model is slightly different from that in Lucas et al. (2014) in order to accommodate the use of an equicorrelation structure later on.

To derive the GAS dynamics for the GHST model, we need the conditional density of y_t, which we parameterize as

$$
\begin{aligned}
p(y_t;\tilde{\Sigma}_t,\gamma,\nu) &= \frac{2\,(\nu/2)^{\nu/2}}{\Gamma(\nu/2)\ |2\pi\,\tilde{\Sigma}_t|^{1/2}} \cdot \frac{K_{(\nu+N)/2}\left(\sqrt{d(y_t)\cdot d(\gamma)}\right) e^{\gamma'\tilde{\Sigma}_t^{-1}(y_t-\tilde{\mu})}}{\left(d(y_t)/d(\gamma)\right)^{(\nu+N)/4}}, && (3)\\
d(y_t) &= \nu + (y_t-\tilde{\mu})'\tilde{\Sigma}_t^{-1}(y_t-\tilde{\mu}), && (4)\\
d(\gamma) &= \gamma'\tilde{\Sigma}_t^{-1}\gamma, \quad \tilde{\mu} = -\frac{\nu}{\nu-2}\gamma, && (5)
\end{aligned}
$$

where $K_a(b)$ is the modified Bessel function of the second kind; see Bibby and Sørensen (2003), The parameters $\gamma = (\gamma_1,\ldots,\gamma_N)' \in \mathbb{R}^N$ and $\nu \in \mathbb{R}^+$ are the skewness and degrees of freedom (or kurtosis) parameter, respectively, while $\tilde{\mu}$ and $\tilde{\Sigma}_t$ denote the location vector and scale matrix, respectively. Note that if y_t has a multivariate GHST distribution with parameters $\tilde{\mu}$, $\tilde{\Sigma}$, γ, and ν as given in (3), then $Ay_t + b$ for some matrix A and vector b also has a GHST distribution, with parameters $A\tilde{\mu}+b$, $A\tilde{\Sigma}A'$, γ, and ν. In particular, the marginal distributions of y_{it} also have a GHST distribution. The GHST density (3) nests symmetric-t ($\gamma = 0$) and multivariate normal ($\gamma = 0$ and $\nu \to \infty$) as a special case.

We parameterize the time-varying matrix $\tilde{\Sigma}_t$ of y_t as in Engle (2002), i.e.,

$$
\tilde{\Sigma}_t = D(f_t)\tilde{R}(f_t)D(f_t), \tag{6}
$$

where f_t is a vector of time varying parameters, $D(f_t)$ is a diagonal matrix holding the scale parameters of y_{it}, and $\tilde{R}(f_t)$ captures the dependence parameters. In our current copula set-up, we use univariate models for $D(f_t)$, and the multivariate model for $\tilde{R}(f_t)$. In Appendix

A.1 we discuss our univariate volatility modeling approach for $D(f_t)$. For the remainder of this section, we concentrate on the matrix $\tilde{R}(f_t)$.

Following Creal et al. (2011, Creal et al. (2013), we endow f_t with score driven (GAS) dynamics using the derivative of the log conditional observation density (3). The transition dynamics for f_t are given by

$$f_{t+1} = \tilde{\omega} + \sum_{i=0}^{p-1} A_i s_{t-i} + \sum_{j=0}^{q-1} B_j f_{t-j}, \tag{7}$$

$$s_t = \mathcal{S}_t \nabla_t, \quad \nabla_t = \partial \ln p(y_t | \mathcal{F}_{t-1}; f_t, \theta)/\partial f_t, \tag{8}$$

where $\tilde{\omega} = \tilde{\omega}(\theta)$ is a vector of fixed intercepts, $A_i = A_i(\theta)$ and $B_j = B_i(\theta)$ are fixed parameter matrices that depend on the vector θ containing all time invariant parameters in the model. The key element in (7) is the use of the scaled score s_t, with scaling function $\mathcal{S}_t$. The following result contains an expression for the score.

Result 1. *Let y_t follow a zero mean GHST distribution $p(y_t; \tilde{\Sigma}_t, \gamma, \nu)$, where the time-varying scale matrix is driven by the GAS model* (7)-(8). *Then the dynamic score is given by*

$$\begin{aligned}
\nabla_t &= \Psi_t' H_t' \text{vec}\left(w_t \cdot (y_t - \tilde{\mu})(y_t - \tilde{\mu})' - 0.5\tilde{\Sigma}_t - \gamma(y_t - \tilde{\mu})' - \breve{w}_t \cdot \gamma\gamma' \right), && (9)\\
w_t &= \frac{\nu + N}{4d(y_t)} - \frac{k'_{0.5(\nu+N)}\left(\sqrt{d(y_t)d(\gamma)}\right)}{2\sqrt{d(y_t)/d(\gamma)}}, && (10)\\
\breve{w}_t &= \frac{\nu + N}{4d(\gamma)} + \frac{k'_{0.5(\nu+N)}\left(\sqrt{d(y_t)d(\gamma)}\right)}{2\sqrt{d(\gamma)/d(y_t)}}, && (11)\\
H_t &= \tilde{\Sigma}_t^{-1} \otimes \tilde{\Sigma}_t^{-1}, \quad \Psi_t = \frac{\partial \text{vec}(\tilde{\Sigma}_t)'}{\partial f_t}, && (12)
\end{aligned}$$

where $k_\nu(\cdot) = \ln K_\nu(\cdot)$ with first derivative $k'_\nu(\cdot)$. The matrices Ψ_t and H_t are time-varying and parameterization specific; both matrices depend on f_t but not on the data y_t.

Proof. See Appendix A.2. □

Result 1 is different from the expressions in Lucas et al. (2014) due to the different parameterization. In our current specification, we model the scale matrix directly in order to fully employ the (block)-equicorrelation structure later on for our conditional law of large numbers result. The result in equation (8) reveals the key feature of the GAS dynamic specification. In essence, the score-driven mechanism takes a Gauss-Newton improvement step for the scale matrix to better fit the most recent observation. Equation (8) shows that f_t reacts to deviations between $\tilde{\Sigma}_t$ and the observed $(y_t - \tilde{\mu})(y_t - \tilde{\mu})'$. The reaction is asymmetric if $\gamma \neq 0$, in which case there is also a reaction to the level $(y_t - \tilde{\mu})$ itself. The reaction to $(y_t - \tilde{\mu})(y_t - \tilde{\mu})'$ is modified by the weight w_t. If $\nu < \infty$, the GHST distribution is fat tailed and the weight decreases in the Mahalanobis distance $d(y_t)$; compare the discussion for the symmetric Student's t case in Creal et al. (2011). This feature gives the model a robustness flavor in that incidental large values of y_t have a limited impact on future volatilities and correlations. The remaining expressions for H_t and Ψ_t only serve to transform the dynamics of the covariance matrix in (6) into the dynamics of the unobserved factor f_t.

To scale the score in (8) we set the scaling matrix S_t equal to the inverse conditional Fisher information matrix of the symmetric Student's t distribution,

$$\mathcal{S}_t = \left\{ \Psi_t' (\tilde{\Sigma}_t^{-1} \otimes \tilde{\Sigma}_t^{-1})' [gG - \mathrm{vec}(\mathrm{I})\mathrm{vec}(\mathrm{I})'] (\tilde{\Sigma}_t^{-1} \otimes \tilde{\Sigma}_t^{-1}) \Psi_t \right\}^{-1}, \tag{13}$$

where $g = (\nu + N)/(\nu + 2 + N)$, and $G = \mathrm{E}[x_t x_t' \otimes x_t x_t']$ for $x_t \sim \mathrm{N}(0, \mathrm{I}_N)$. Zhang et al. (2011) demonstrate that this results in a stable model that outperforms alternative models if the data are fat-tailed and skewed.

2.3 Dynamic (Block)-Equicorrelation (DECO) Structure

As we want to use our model in the context of a large cross-sectional dimension to describe the joint (tail) risk dynamics in a large system of financial institutions, we refrain from modeling all dependence parameters in $\tilde{R}(f_t)$ individually. Instead, we adopt the approach of Engle and Kelly (2012) and impose a block-equicorrelation (block-DECO) structure on the matrix $\tilde{R}(f_t)$. By limiting the number of free parameters, we considerably facilitate the estimation process while we can still capture dynamic patterns in the dependence structure amongst financial firms, particularly in times of stress.

For the (single block) DECO structure, we assume that $\tilde{\Sigma}_t$ takes the form

$$\tilde{\Sigma}_t = (1 - \rho_t^2)\mathrm{I}_N + \rho_t^2 \ell_N \ell_N', \tag{14}$$

where $\rho_t \in (0,1)$, and ℓ_N is a $N \times 1$ vector of ones. Using the specific form of $\tilde{\Sigma}_t$ in (14), the expressions for Ψ_t and H_t and Result 1 simplify considerably. We summarize this in the following result.

Result 2 (single block DECO)**.** *If* $\tilde{\Sigma}_t = (1-\rho_t^2)\mathrm{I}_N + \rho_t^2 \ell_N \ell_N'$, *and* $\rho_t = (1+\exp(-f_t))^{-1}$, *we obtain*

$$\Psi_t = \frac{\partial \mathrm{vec}(\tilde{\Sigma}_t)'}{\partial f_t} = (\ell_{N^2} - \mathrm{vec}(\mathrm{I}_N)) \, \frac{2\exp(-f_t)}{(1+\exp(-f_t))^3}. \tag{15}$$

Proof. See Appendix A.3. □

We can easily generate the equicorrelation structure in (14) from model (1) by writing

$$y_{it} = (\varsigma_t - \mu_\varsigma)\, \gamma_i + \sqrt{\varsigma_t} \left(\rho_t \, \kappa_t + \sqrt{1-\rho_t^2} \tilde{\epsilon}_{it} \right), \tag{16}$$

where κ_t and $\tilde{\epsilon}_{it}$ are two independent standard normal random variables. The logistic parameterization $\rho_t = (1+\exp(f_t))^{-1}$ forces the correlation parameter to be in the unit interval, irrespective of the value of $f_t \in \mathbb{R}$. Though the original equicorrelation specification of Engle and Kelly (2012) also allows for (slightly) negative equicorrelations, such values are typically unrealistic in the type of applications we consider later on. The parameterization with equicorrelation parameter $\rho_t^2 > 0$ therefore suffices for our current purposes.

The restriction of a single correlation parameter characterizing the entire scaling matrix $\tilde{\Sigma}_t$ might be too restrictive empirically, particularly if we want to consider differences in dependence between financial firms in different countries. For example, in the context of the euro area sovereign debt crisis we might want to allow for different dependence features between firms in stressed and non-stressed countries. For two blocks containing N_1 and N_2 firms, respectively, our block-DECO specification is given by

$$\tilde{\Sigma}_t = \begin{bmatrix} (1-\rho_{1,t}^2)\mathrm{I}_{N_1} & 0 \\ 0 & (1-\rho_{2,t}^2)\mathrm{I}_{N_2} \end{bmatrix} + \begin{pmatrix} \rho_{1,t}\ell_{N_1} \\ \rho_{2,t}\ell_{N_2} \end{pmatrix} \cdot \begin{pmatrix} \rho_{1,t}\ell_{N_1}' & \rho_{2,t}\ell_{N_2}' \end{pmatrix}. \tag{17}$$

The specification in (17) is somewhat more restrictive than the block-equicorrelation structure laid out in Engle and Kelly (2012). The main advantage, however, is that the form in (17) preserves the Vasicek (1987) single factor credit risk structure of y_t (conditional on ς_t).

This feature is important for the conditional law of large numbers result in Section 3. This result in turn allows us to compute joint and conditional risk measures fast and efficiently in large dimensions, precisely when standard simulation methods quickly become inefficient.[3] Using the block-DECO structure (17) we obtain the following result.

Result 3 (two-block DECO). *If $\tilde{\Sigma}_t$ is given by* (17) *with $\rho_{j,t} = (1+\exp(-f_{j,t}))^{-1}$ for $j = 1, 2$, then the time varying factor $f_t = (f_{1,t}, f_{2,t})' \in \mathbb{R}^{2\times 1}$ follows the system* (9)–(12)*, with*

$$\Psi_t = \frac{\partial \mathrm{vec}(\tilde{\Sigma}_t)'}{\partial f_t} = \frac{\partial \mathrm{vec}(\tilde{\Sigma}_t)'}{\partial \rho_t} \frac{d\rho_t'}{df_t}, \tag{18}$$

$$\frac{d\rho_t'}{df_t} = \begin{pmatrix} \frac{\exp(-f_{1,t})}{(1+\exp(-f_{1,t}))^2} & 0 \\ 0 & \frac{\exp(-f_{2,t})}{(1+\exp(-f_{2,t}))^2} \end{pmatrix}, \tag{19}$$

$$\begin{aligned} \frac{\partial \mathrm{vec}(\tilde{\Sigma}_t)'}{\partial \rho_t} &= \left(\mathrm{vec}\begin{pmatrix} \mathrm{I}_{N_1} & 0 \\ 0 & 0 \end{pmatrix}, \mathrm{vec}\begin{pmatrix} 0 & 0 \\ 0 & \mathrm{I}_{N_2} \end{pmatrix} \right) \cdot \begin{pmatrix} -2\rho_{1,t} & 0 \\ 0 & -2\rho_{2,t} \end{pmatrix} \\ &+ \left(\begin{pmatrix} \rho_{1,t}\ell_{N_1} \\ \rho_{2,t}\ell_{N_2} \end{pmatrix} \otimes \mathrm{I}_N + \mathrm{I}_N \otimes \begin{pmatrix} \rho_{1,t}\ell_{N_1} \\ \rho_{2,t}\ell_{N_2} \end{pmatrix} \right) \cdot \left(\begin{pmatrix} \ell_{N_1} \\ 0 \end{pmatrix}, \begin{pmatrix} 0 \\ \ell_{N_2} \end{pmatrix} \right), \end{aligned} \tag{20}$$

where $\rho_t = (\rho_{1,t}, \rho_{2,t})'$ and $N = N_1 + N_2$.

Proof. See Appendix A.3. □

We can introduce further flexibility to the model by extending the support of $\rho_{1,t}$ and $\rho_{2,t}$ from $(0, 1)$ to $(-1, 1)$ by defining $\rho_{j,t} = (\exp(f_{j,t}) - 1)/(\exp(f_{j,t}) + 1)$ for $j = 1, 2$. The advantage of this extension is that the correlations between blocks can now become negative, whereas the within block correlation remains positive. For the empirical application in Section 4, however, this extension is not needed.

We can also easily generalize the 2-block specification to an m-block DECO structure. The corresponding equations resemble those in Result 3. Rather than providing the (lengthy) expressions in the main text, we refer to Appendix A.3 for the precise formulations. These formulations are used in our empirical analysis in Section 4, where we also consider a 3-block equicorrelation specification.

[3] We demonstrate in Section 4.2 based on $N = 10$ firms that the tail risk measurements obtained from applying (14) (or (17)) are close to those based on a full correlation matrix analysis.

2.4 Parameter estimation

We can estimate the static parameters θ of the dynamic GHST model by standard maximum likelihood procedures. Likelihood estimation is straightforward as the likelihood function is known in closed form using a standard prediction error decomposition. Deriving the asymptotic behavior for time varying parameter models with GAS dynamics is non-trivial. We refer to Blasques et al. (2012, Blasques et al. (2014a, Blasques et al. (2014c) and Lucas and Silde (2014) for details.

As mentioned earlier, we split the estimation problem into two parts by adopting a copula perspective. As a result, the number of parameters that need to be estimated in each step is reduced substantially. In addition, the copula perspective has the advantage that we can add more flexibility to modeling the marginal distributions. For example, when working with a multivariate GHST density, all marginal distributions must have the same kurtosis parameter ν. By adopting a copula perspective, we can relax this restriction.

The two stages of the estimation process can be summarized as follows. In a first step, we estimate univariate dynamic GHST models using the equity returns for each firm i based on the maximum likelihood approach as discussed in Appendix A.1. Using the estimated univariate models with parameters are $\tilde{\mu}_{it}$, $\tilde{\sigma}_{it}$, γ_i, and ν_i, we transform the observations into their probability integral transforms $u_{it} \in [0,1]$. In the second step, we estimate the matrix $\tilde{\Sigma}_t = \tilde{R}_t$ as parameterized in Section 2.3 using the probability integral transforms u_{it} constructed in the first step. The GHST copula parameters are 0, $\tilde{R}_t$, $\gamma \cdot (1,\ldots,1)'$ for $\gamma \in \mathbb{R}$, and ν. The static parameters to be estimated include the parameters $\tilde{\omega}$, A_j, and B_j of the dynamic equation (7).

3 Joint and conditional risk measures

A direct method to compute joint and conditional default probabilities is based on Monte Carlo simulations of firms' asset values. For example, we can generate many paths for the joint evolution of all the y_{it}s and check how many simulations lie in a joint distress region of the the type $\{y_t \,|\, y_{jt} < y^*_{jt} \; \forall j \in J\}$ for some set of firms $J \subset \{1,2,\ldots,N\}$, where y^*_{jt}

denotes the default threshold for firm j. While simulating risk measures in this way is conceptually easy, such a simulation based approach quickly becomes inefficient if the cross sectional dimension of the data and the number of firms considered in the set J grow large: because marginal default probabilities are typically small, we would need a large number of simulations to obtain realizations of joint defaults, particularly if 3, 4, or even more joint defaults are considered.

To overcome the computational inefficiency of simple simulation based risk assessments, we define joint and conditional risk measures and demonstrate how to compute them in a fast and reliable way based on an application of a conditional law of large numbers (cLLN). The use of a cLLN in the credit risk context has been popularized by Vasicek (1987) and studied further in for example Gordi (2000, 2003) and Lucas et al. (2001, 2003). We show that the cLLN in our setting already provides reliable results for low-dimensional cases such as $N = 10$. While we focus on financial sector firms, the derivations presented in this section are general.

We exploit the (block-)equicorrelation structure in (14) and (17) to obtain reliable alternative risk measures that can be evaluated semi-analytically. We define the joint tail risk measure (JRM) as the time-varying probability that a certain fraction of firms defaults over a pre-specified period. Let $c_{N,t}$ denote the fraction of financial firm defaults at time t, e.g., $c_{N,t} = 5\%$, with

$$c_{N,t} = \frac{1}{N}\sum_{i=1}^{N} 1\{y_{it} < y_{it}^*\}. \tag{21}$$

Since the indicators $1\{y_{it} < y_{it}^*\}$ are conditionally independent given κ_t and ς_t, we can apply a conditional law of large numbers to obtain

$$c_{N,t} \approx \frac{1}{N}\sum_{i=1}^{N} \mathrm{E}[1\{y_{it} < y_{it}^*\} \mid \kappa_t, \varsigma_t] = \frac{1}{N}\sum_{i=1}^{N} \mathrm{P}[y_{it} < y_{it}^* \mid \kappa_t, \varsigma_t] := C_{N,t}, \tag{22}$$

for large N. As mentioned earlier, such cLLNs are routinely applied in credit risk settings; see for example Vasicek (1987), Gordy(2000, 2003), and Lucas et al. (2001). Note that

$$\mathrm{P}[y_{it} < y_{it}^* | \kappa_t, \varsigma_t] = \Phi\left(\frac{y_{it}^* - (\varsigma_t - \mu_\varsigma)\,\gamma_i - \sqrt{\varsigma_t}\,\rho_t\kappa_t}{\sqrt{\varsigma_t\,(1-\rho_t^2)}}\right), \tag{23}$$

where $\Phi(\cdot)$ denotes the cumulative standard normal distribution. Also note that $C_{N,t}$ is a function of the random variables κ_t and ς_t only, and not of $\tilde{\epsilon}_{it}$ in (16). We now define the joint tail risk measure (JRM) as

$$p_t = \mathrm{P}(C_{N,t} > \bar{c}) = \mathrm{P}(C_{N,t}(\kappa_t, \varsigma_t) > \bar{c}), \tag{24}$$

i.e., the probability that the fraction of credit portfolio defaults $C_{N,t}$ exceeds the threshold $\bar{c} \in [0, 1]$. The fraction of portfolio defaults $C_{N,t}$ is a (possibly complicated) function of its two arguments κ_t and ς_t. When seen as a function of κ_t for given ς_t, however, we note that $C_{N,t}$ is monotonically decreasing in κ_t. This is intuitive: an increase in κ_t (for instance due to improved business cycle conditions) implies less defaults in the portfolio and vice versa. We exploit this to efficiently compute unique threshold levels $\kappa^*_{t,N}(\bar{c}, \varsigma^{(g)})$ for a number of grid points $\varsigma^{(g)}$, $g = 1, \ldots, G$. This can be done by solving the equation $C_{N,t}(\kappa^*_{t,N}(\bar{c}, \varsigma^{(g)}), \varsigma^{(g)}) = \bar{c}$ numerically for the threshold value $\kappa^*_{t,N}(\bar{c}, \varsigma^{(g)})$ for each grid point $\varsigma^{(g)}$. Given a grid of threshold values, we can then use standard numerical integration techniques to efficiently compute the joint default probability

$$p_t = \mathrm{P}(C_{N,t} > \bar{c}) = \int \mathrm{P}(\kappa_t < \kappa^*_{t,N}(\bar{c}, \varsigma_t)) p(\varsigma_t) \mathrm{d}\varsigma_t, \tag{25}$$

effectively integrating out a well-behaved (inverse gamma) random variable.

Our second measure is a conditional tail risk measure (CRM). Let

$$C^{(-i)}_{N-1,t} = (N-1)^{-1} \sum_{j \neq i} \mathrm{P}[y_{jt} < y^*_{jt} \mid \kappa_t, \varsigma_t],$$

be the approximate fraction of defaulted companies excluding firm i using the cLLN approximation, and let $\bar{c}^{(-i)}$ denote our threshold value for this fraction. We define the CRM as the probability of $C^{(-i)}_{N-1,t}$ exceeding $\bar{c}^{(-i)}$ conditional on the default of firm i, i.e.,

$$\begin{aligned}
\mathrm{P}\Big(C^{(-i)}_{N-1,t} > \bar{c}^{(-i)} \;\Big|\; y_{it} < y^*_{it}\Big) &= p_{it}^{-1} \cdot \mathrm{P}(C^{(-i)}_{N-1,t} > \bar{c}^{(-i)} \;,\; y_{it} < y^*_{it}) \\
&= p_{it}^{-1} \cdot \int \mathrm{P}\left(\kappa_t < \kappa^*_{N-1,t}(\bar{c}^{(-i)}, \varsigma_t) \;,\; y_{it} < y^*_{it} \;\middle|\; \varsigma_t\right) \; p(\varsigma_t) \mathrm{d}\varsigma_t \\
&= p_{it}^{-1} \cdot \int \Phi_2(\kappa^*_{N-1,t}(\bar{c}^{(-i)}, \varsigma_t) \;,\; y^{**}_{it}(\varsigma_t) \;;\; \rho_t) \; p(\varsigma_t) \mathrm{d}\varsigma_t,
\end{aligned} \tag{26}$$

where $y_{it}^{**}(\varsigma_t) = (y_{it}^{*} - (\varsigma_t - \mu_\varsigma)\gamma_i)/\sqrt{\varsigma_t}$, and $\Phi_2(\cdot, \cdot; \rho_t)$ denotes the cumulative distribution function of the bivariate normal with standard normal marginals and correlation parameter ρ_t. To obtain the last equality in (26), note that the GHST distribution becomes Gaussian conditional on ς_t. The conditional probability (26) is a time-varying and higher-frequency extension of the multivariate extreme spillovers measure of Hartmann, Straetmans, and De Vries (2004, 2007).

Both the joint tail risk measure (JRM) in equation (25) and the conditional tail risk measure (CRM) in equation (26) can be computed based on a simple 1-dimensional numerical integration over the positive real line. As a result, both measures can be computed quickly. We also note that it is straightforward to add exposure weights e_i to the definition of $c_{N,t}$ in (21). The computations in that case remain equally efficient. If the exposures are very unevenly distributed, however, the approximation error of the cLLN in (22) might increase. To mitigate such an effect, one could try to implement a second order expansion using a conditional central limit theorem rather than a cLLN only. Finally, we note that the model is easily extended to fit the m-block DECO structure explained in Section 2.3. The fact that $\rho_{i,t}$ parameters are different between blocks does not distort the one-factor credit risk structure of the current set-up, and all computations remain of similar structure and speed.

4 Empirical application: euro area financial sector risk during the financial and sovereign debt crisis

We apply our model to euro area financial firms. In a first analysis, we focus on $N = 10$ large firms, where each firm is headquartered in a different euro area country. The small cross-sectional dimension allows us to benchmark the dynamic GHST block-DECO model against a model with a fully specified time varying correlation matrix and to investigate the sensitivity of the joint tail risk measure (JRM) and the conditional tail risk measure (CRM) to the equicorrelation assumption. Subsequently, we focus on a large scale application based on $N = 73$ euro area financial firms.

4.1 Equity and EDF data

Our 73 listed financial firms are located in 11 euro area countries: Austria (AT), Belgium (BE), Germany (DE), Spain (ES), Finland (FI), France (FR), Greece (GR), Ireland (IE), Italy (IT), the Netherlands (NL), and Portugal (PT). We selected these firms as the subset of financial sector firms that (i) are, as of 2011Q1, listed as a component of the STOXX Europe 600 index, a broad European equity price index, and (ii) are headquartered in the euro area. For each firm, we observe demeaned weekly equity returns. Equity data are obtained from Bloomberg. The sample comprises large commercial banks as well as large financial non-banks such as insurers and investment companies. The total panel covers 762 weeks from January 1999 to August 2013. The panel is unbalanced in that some data are missing in the first part of the sample. Dealing with missing values is straightforward in our framework, as long as the data are missing completely at random: the score steps only account for the joint density of the observed values. For the marginal default probabilities p_{it}, we use one year ahead expected default frequencies (EDF) obtained from Moody's Analytics. Such EDFs are widely-used measures of time-varying one year ahead marginal default probabilities (Duffie et al. (2007)).

4.2 $N = 10$: Ten large banking groups

In our first application, we select a geographically diversified sub-sample of ten large financial firms from ten euro area countries: Erste Bank Group (AT), Dexia (BE), Deutsche Bank (DE), Santander (ES), BNP Paribas (FR), National Bank of Greece (GR), Bank of Ireland (IE), UniCredito (IT), ING (NL), and Banco Comercial Portugues (PT). This subsample contains no missing observations. The descriptive statistics in Table 1 indicate that the weekly equity returns corresponding to our subsample of ten financial firms are significantly negatively skewed and fat-tailed, suggesting that a dynamic GHST model is appropriate. We distinguish different sets of financial firms based on their country location because of the mutual dependence of bank and sovereign risk (as well as the market fragmentation due to this link) that was an acknowledged feature of the euro area sovereign debt crisis, see for

Table 1: Sample descriptive statistics

The table reports descriptive statistics for $N = 10$ weekly equity returns between January 1999 and August 2013. The sample mean values are all close to zero. All excess kurtosis and skewness coefficients are significantly different from 0 at the 5% significance level.

	Median	Std.Dev.	Skewness	Kurtosis	Minimum	Maximum
Bank of Ireland	0.004	0.099	-0.614	14.736	-0.658	0.581
Banco Comercial Portugues	0.004	0.049	-0.375	6.753	-0.284	0.230
Santander	0.002	0.049	-0.558	7.289	-0.261	0.212
UniCredito	0.001	0.084	-0.235	15.968	-0.705	0.613
National Bank of Greece	0.003	0.061	-1.253	12.909	-0.475	0.292
BNP Paribas	0.002	0.056	-0.364	10.344	-0.367	0.339
Deutsche Bank	0.000	0.059	-0.489	16.145	-0.529	0.398
Dexia	0.008	0.087	-0.569	13.735	-0.529	0.494
Eerste Group Bank	0.002	0.061	-1.143	16.100	-0.552	0.296
ING	0.004	0.069	-1.319	13.358	-0.546	0.290

example ECB (2012b) and Coeuré (2013).

We consider four different models. All models use the score (GAS) dynamics for time varying volatilities and correlations, but the structure of their correlation matrices differs. As we use a copula approach, all models share the same structure for the univariate volatility models; we refer to the Appendix A.1 for more details. Without showing the respective volatility plots for space considerations, we report that all ten financial firms exhibit periods of high equity volatility. A pronounced period of high volatility starts on 15 September 2008 with the bankruptcy of Lehman Brothers. From 2010-12 the euro area sovereign debt crisis also strongly affects equity volatilities. Volatility tends to increase more for financial firms headquartered in stressed countries (Greece, Ireland, and Portugal, starting in 2011 also Spain and Italy) compared to other relatively less- or non-stressed countries in the euro area (such as Austria, Belgium, Germany, France, and The Netherlands).

Our first model uses a full correlation matrix with GAS dynamics. Following the multivariate DCC model of Engle (2002), the GAS GHST copula model is highly parsimonious and uses a scalar A and B to drive the correlation dynamics. In addition, it uses a common scalar skewness parameter γ in the GHST copula. The full GAS correlation model contains 45 pairwise correlation coefficients, and thus 45 dynamic factors. Standard correlation targeting is used to estimate the intercepts in the transition equation for the correlations.

Table 2: Multivariate model estimates for filtered data

Parameter estimates for our multivariate GAS-GHST models of financial firms' equity returns. Columns 2 to 5 refer to our copula model for $N = 10$ financial firms. Columns 6 to 7 refer to the modeling of the full set of N=73 financial firms. Univariate GAS-GHST models are used for the modeling of marginal volatilities before estimating the dynamic equicorrelation copula models. For the 2-block model, we distinguish between financial firms from stressed countries (Greece, Portugal, Spain, Italy, Ireland) and firms from the remaining non-stressed countries. In the 3-block model, we distinguish between financial firms from smaller stressed countries (Greece, Portugal, Ireland), firms from larger stressed countries (Spain, Italy), and firms from the remaining non-stressed countries. The 2$*$-block model merges the firms from non-stressed and large stressed countries (Spain, Italy), and only assigns a separate dynamic correlation to financial firms headquartered in small stressed countries (Greece, Portugal, Ireland). AICc denotes the finite-sample corrected version of the AIC of Hurvich and Tsai (1989).

	10 firms				73 firms	
	GAS-DECO[1]	GAS-DECO[2]	GAS-DECO[3]	GAS-DECO[2$*$]	GAS-DECO[1]	GAS-DECO[2]
A	0.219	0.116	0.085	0.119	0.522	0.236
	(0.068)	(0.023)	(0.015)	(0.022)	(0.088)	(0.028)
B	0.979	0.989	0.991	0.989	0.978	0.995
	(0.018)	(0.008)	(0.006)	(0.008)	(0.017)	(0.003)
ω_1	0.585	0.249	0.208	-0.238	0.190	-0.882
	(0.186)	(0.276)	(0.304)	(0.370)	(0.302)	(0.314)
ω_2		0.794	0.194	0.856		0.035
		(0.248)	(0.370)	(0.214)		(0.311)
ω_3			0.810			
			(0.222)			
ν	17.095	17.554	17.625	17.867	32.808	26.234
	(1.761)	(0.005)	(0.007)	(0.004)	(1.795)	(0.925)
γ_1	-0.393	-0.441	-0.435	-0.468	-0.229	-0.223
	(0.093)	(0.000)	(0.001)	(0.000)	(0.066)	(0.058)
γ_2		-0.361	-0.445	-0.344		-0.239
		(0.000)	(0.001)	(0.000)		(0.043)
γ_3			-0.366			
			(0.001)			
Log-lik	1499.6	1536.4	1529.9	1610.4	11010.8	11014.5
AIC	-2989.2	-3058.7	-3041.9	-3206.8	-22011.5	-22014.9
BIC	-2956.8	-3013.4	-2983.6	-3161.4	-21997.6	-21995.4
AICc	-2989.1	-3058.6	-3041.6	-3206.6	-22011.4	-22014.8

We use the full model to benchmark three different GAS-DECO specifications with 1, 2 and 3 blocks, respectively. In the 2-block model, we distinguish between financial firms in five countries under pronounced stress during the sovereign debt crisis (Greece, Ireland, Italy, Portugal, Spain) and firms from non- or less-stressed countries. In the 3-block model, we distinguish financial firms from smaller stressed countries (Greece, Portugal, Ireland), larger stressed countries (Spain, Italy), and the remaining countries. This modeling choice reflects the notion that the sovereign debt crisis spread from Greece, Ireland, and Portugal to Italy and Spain only at a later stage of the crisis, see Eser et al. (2012), Eser and Schwaab (2013), and ECB (2014).

Table 2 provides the parameter estimates as well as a set of model selection criteria. The left columns in Table 2 suggest that the correlations are highly persistent for all specifications considered, as the B parameters are all close to unity. The unconditional correlation levels, as captured by the parameters ω_i, are higher for the stressed countries, in particular the smaller stressed countries (ω_3). If we look at the model selection criteria AIC, BIC, or AICc, the GAS-DECO[2*] model is preferred. In this model the financial firms from Ireland, Portugal, and Greece have their own dynamic correlation parameter separate from the other countries (including Italy and Spain).

Figure 1 plots the estimated dynamic correlations. The top left panel plots the average pairwise correlations of each firm with the other (nine) firms. These correlation estimates are based on the modeling of a full correlation matrix with 45 time varying parameters. The estimates strongly suggest a pronounced commonality in the correlation dynamics over time. For instance, all correlations tend to increase over the sample period, possibly reflecting gradual financial integration and economic convergence in the euro area after the inception of the euro in 1999. All correlations remain elevated during the financial crisis from 2008-2010. Finally, correlations come down from high levels to some extent during the euro area sovereign debt crisis in 2011-2012.

Such common correlation dynamics can be captured simply and conveniently by a 1-block DECO structure. The top right panel in Figure 1 plots the GAS 1-block equicorrelation over time. Due to the structure of the model, the dynamics are much clearer. There appears to be a drop in correlations after the burst of the dotcom bubble, possibly due to the different exposures of the different euro area financial firms to U.S. equity markets and the subsequent recession. The maximum correlation is reached in mid-2010, at a time when Greece, Ireland, and Portugal needed the assistance of third parties such as the EU and the IMF, see ECB (2012a).

The common picture changes somewhat when we allow for different correlations among financial firms located in stressed and non-stressed countries, respectively. The left panel in the middle row of Figure 1 plots the dynamic correlation estimates for these two groups. The first group contains the Bank of Ireland, Banco Comercial Portugues, Santander, UniCredito and the National Bank of Greece. The second group includes BNP Paribas, Deutsche Bank,

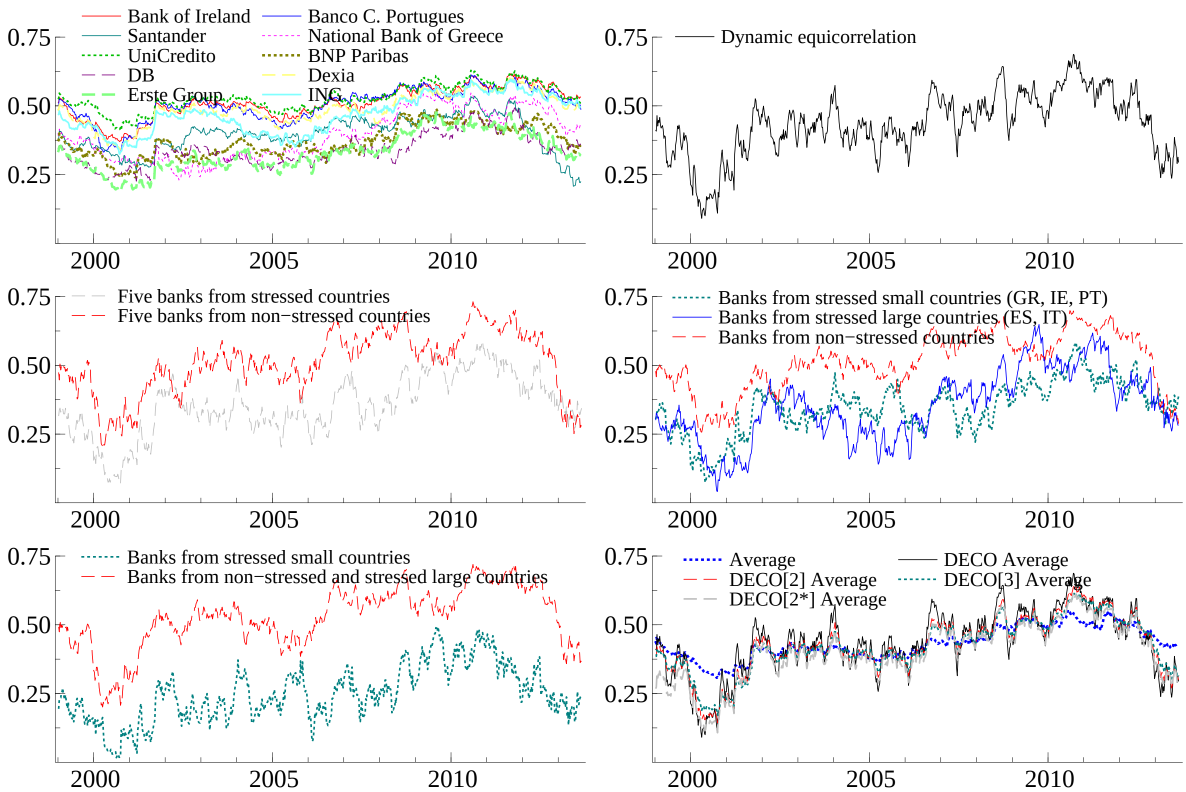

Figure 1: Filtered correlation estimates for $N = 10$ financial firms

The top left panel plots the average correlation estimate with the nine other firms for each financial firm, using the full correlation model. The top right panel plots the dynamic correlations for the 1-block DECO model. The middle left panel reports the block equicorrelation estimates from a 2-block DECO model. The middle right panel plots three block equicorrelations from a 3-block DECO model. The bottom left panel plots correlation estimates from a 2-block model which pools over banks from non-stressed and large stressed countries. The bottom right panel plots the average correlations over all 45 pairs for the full correlation matrix model, for the 1-block, 2-block, and 3-block DECO models.

Dexia, Erste Bank Group, and ING. The overall dependence dynamics are similar. However, and perhaps surprisingly, the correlation between financial firms from non-stressed countries lies substantially above that of financial firms from countries that became stressed during the sovereign debt crisis. This pattern holds in particular before the onset of the financial and debt crisis in 2008, and may therefore be related to different degrees of financial integration rather than to shared exposure to heightened market turmoil in a crisis (ECB (2012a)).

The middle right panel plots the correlation estimates for the 3-block DECO model. The correlation between financial firms from non-stressed countries continues to lie above that of financial firms from countries that became stressed during the debt crisis. In addition, the correlation dynamics are again fairly similar across the different sets of firms. The bottom left panel plots the correlation estimates for the 2-block DECO model that pools across firms in non-stressed and stressed large countries while allowing for different correlations for the three firms located in Greece, Ireland, and Portugal. While the overall correlation dynamics are similar, the maximum correlation is achieved earlier in the second stressed group (in 2009-2010). This is intuitive given that Ireland, Greece and Portugal were the first euro area countries that needed economic assistance during the crisis.

The bottom right panel compares the average correlation levels across all 45 pairs for different models. The average correlations are similar across all models. Only relatively minor deviations are observed. The pairwise correlation estimates are relatively lower for the full correlation matrix specification from 2010 to mid-2011. The converse holds from late 2012 onwards, after policy reactions of the ECB had calmed the markets. We conclude that the equicorrelation model reliably estimates the salient trend in correlation dynamics. Correlations from the equicorrelation specifications exhibit larger and more intuitive time series variation than the average correlation from the unrestricted model.

We can now use the different dependence models to compute the joint tail risk measure (JRM) and conditional tail risk measure (CRM) introduced in Section 3. We use the default thresholds obtained by inverting the GHST distribution function at the observed EDF levels. Given the small cross sectional dimension of the model, we can benchmark the adequacy of the cLLN approximation compared to a brute force simulation based approach to computing

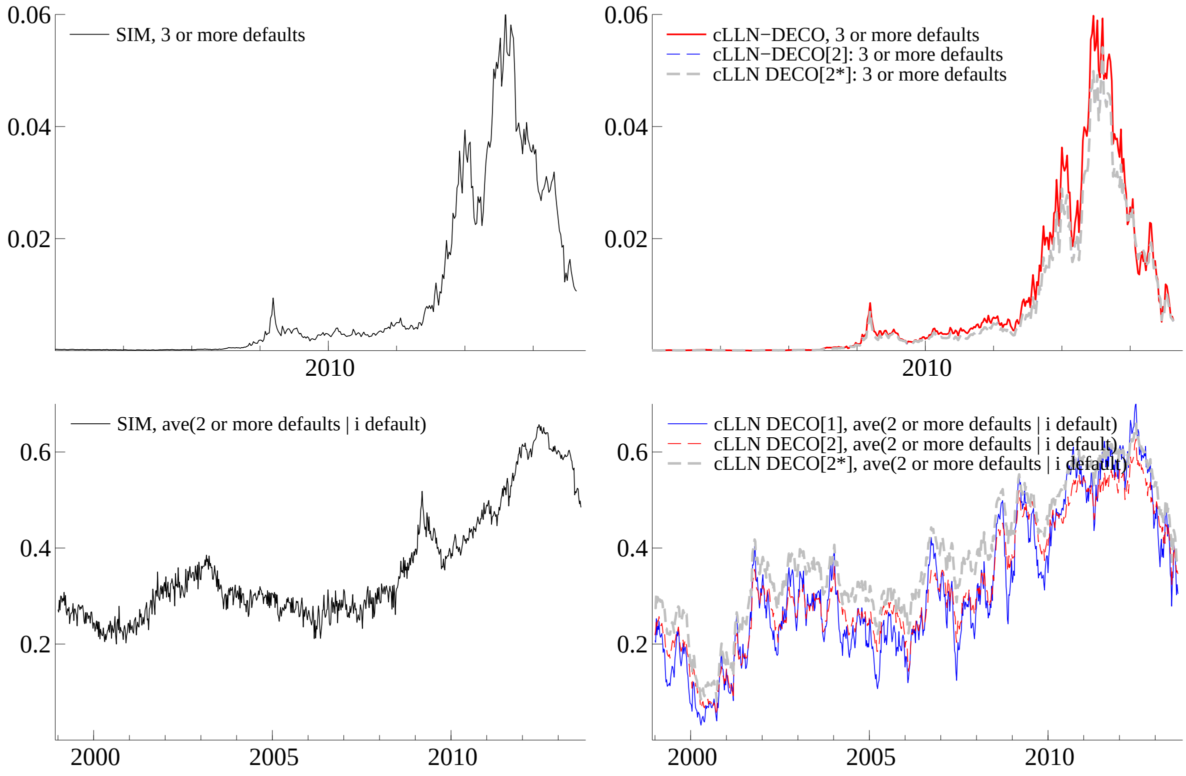

Figure 2: Joint and conditional tail risk measures based on simulation and cLLN approximation

We report the joint tail risk measure (JRM, top left and right panels) defined in (25) for three or more defaults out of ten, and the average conditional tail risk measure (CRM, bottom left and right panels). The CRM is defined in (26) and here taken as the probability of 2 or more (out of 9 possible) credit events given a credit event for a given financial firm, averaged over all ten firms. The risk measures are either computed using 500,000 simulations at each point in time t and a full correlation matrix (left top and bottom panels), or alternatively using the cLLN approximation as discussed in Section 3 for the DECO and block-DECO models (right top and bottom panels).

the JRM and CRM. For the simulation based computations, we use 500,000 simulations at each time t and count the number of firms under stress. The semi-analytical calculations based on the cLLN by contrast are fast and less cumbersome than the simulation based method. Figure 2 reports the JRM for three or more defaults out of ten firms, as well as the average CRM of all firms in the sample.

The left and right panels of Figure 2 demonstrate that the dynamic patterns and overall levels of the joint (top two panels) and conditional tail risk measures (bottom two panels) are similar irrespective of the computation method used. Regarding the top panels, the cLLN approximated JRM appears to slightly understate the risk in good times and to slightly overstate the risk during the crisis period around 2012. The proximity of the two time series, however, is encouraging for using the cLLN approximation and DECO assumption in the larger system of $N = 73$ financial firms. Also the CRM in the bottom two panels reveals that the DECO assumption and cLLN approximation work well for the conditional risk measure compared to the simulation approach. The overall time series patterns for both series are again similar. The simulation based approach of the conditional probability is substantially noisier particularly if the joint risk is low, i.e., up to mid 2009. In particular, we see the drop and subsequent rise in conditional probabilities during the unfolding of the financial crisis, and further increases during the euro area sovereign debt crisis. Under the conditional LLN approximations, the equicorrelation models provide similar outcomes for the risk measures regardless of the number of blocks used in the estimation.

Based on our small sample study with ten firms, we conclude that the full correlation model and the block equicorrelation models lead to a similar time varying pattern for the joint and conditional risk measures. The cLLN works well even when the data dimension is relatively small. Finally, the simulation based approach can suffer from sizable simulation noise in non-crisis periods (when marginal default probabilities are low), while no such problems are encountered for the cLLN based approximation.

4.3 Large N: The euro area financial sector

In this section we apply our new joint and conditional tail risk measures to the full panel of 73 financial sector firms. The sample contains commercial banks as well as financial non-banks such as insurers and investment companies.[4] Table 3 reports descriptive statistics for all 73 firms' equity returns. The GHST model seems appropriate given the pronounced skewness and kurtosis features of the data. As mentioned before, the GAS dynamics automatically account for the presence of missing values. Each firm starts to contribute to the

[4]Freezing the set of firms as the constituents of a broad based equity index in 2011Q1 means that we may underestimate total euro area financial sector risk prior to this date (due to sample selection; weaker firms may have dropped out of the index by then). While this concern should be kept in mind, it is unlikely to be large, as most financial institutions under stress during the financial crisis continued to operate, also due to substantial government aid and the extension of public sector guarantees. Sample selection is no issue after 2011Q1.

Table 3: Sample summary statistics for all 73 financial institutions

The table reports sample moments across all 73 institutions included in the empirical application. For example, the row labeled '*skewness*' contains the mean and standard deviation of the skewness statistic across all 73 firms, followed by the minimum, 25th, 50th, and 75th percentile, and the maximum.

	Mean	Std. Dev.	Minimum	25%	50%	75%	Maximum
Count	717.027	116.360	196.000	762.000	762.000	762.000	762.000
Mean	0.000	0.000	0.000	0.000	0.000	0.000	0.000
Std. Dev.	0.056	0.020	0.025	0.043	0.049	0.061	0.113
Skewness	-0.812	1.937	-12.062	-0.836	-0.406	-0.218	1.894
Kurtosis	18.046	38.466	3.694	6.770	10.127	14.261	266.259

equicorrelation dynamics once it enters the sample.

Figure 3 plots the dynamic correlations estimates based on the same models as described in Section 4.2, but now estimated for the full sample of $N = 73$ firms. The equicorrelations (top left) range from low values of approximately 0.1 in 2000 to values as high as 0.6 towards the start of the euro area sovereign debt crisis in 2010. Using the two block structure (top right), there appear to be little differences between financial firms from stressed versus non-stressed countries, except during the peak of the sovereign debt crisis in 2011–2012. Interestingly, institutions from non-stressed countries appear to have a higher degree of clustering. This difference may be due to the heterogeneous nature of the different financial institutions in the different stressed countries.

The bottom left panel of Figure 3 introduces further heterogeneity by modeling the dynamic correlation for firms from Greece, Ireland, and Portugal on the one hand and Italy and Spain on the other hand. Again, Ireland, Greece, and Portugal entered the sovereign debt crisis earlier, and were relatively more stressed compared to Spain and Italy. We see a lower level of correlation among financial institutions from the first group of smaller stressed countries. The correlation rises after the financial crisis up to the start of 2010, and then decreases to pre-crisis levels around 2012. By contrast, the correlation for financial firms from Italy and Spain starts to rise earlier, peaks higher, and remains (together with the correlations of the non-stressed countries) high until the end of the sample. If we consider the average correlations across all $73(73-1)/2 = 2628$ pairs (lower right), the picture emerging from all three models is similar.

We compute the financial tail risk measures using the cLLN approximation from Sec-

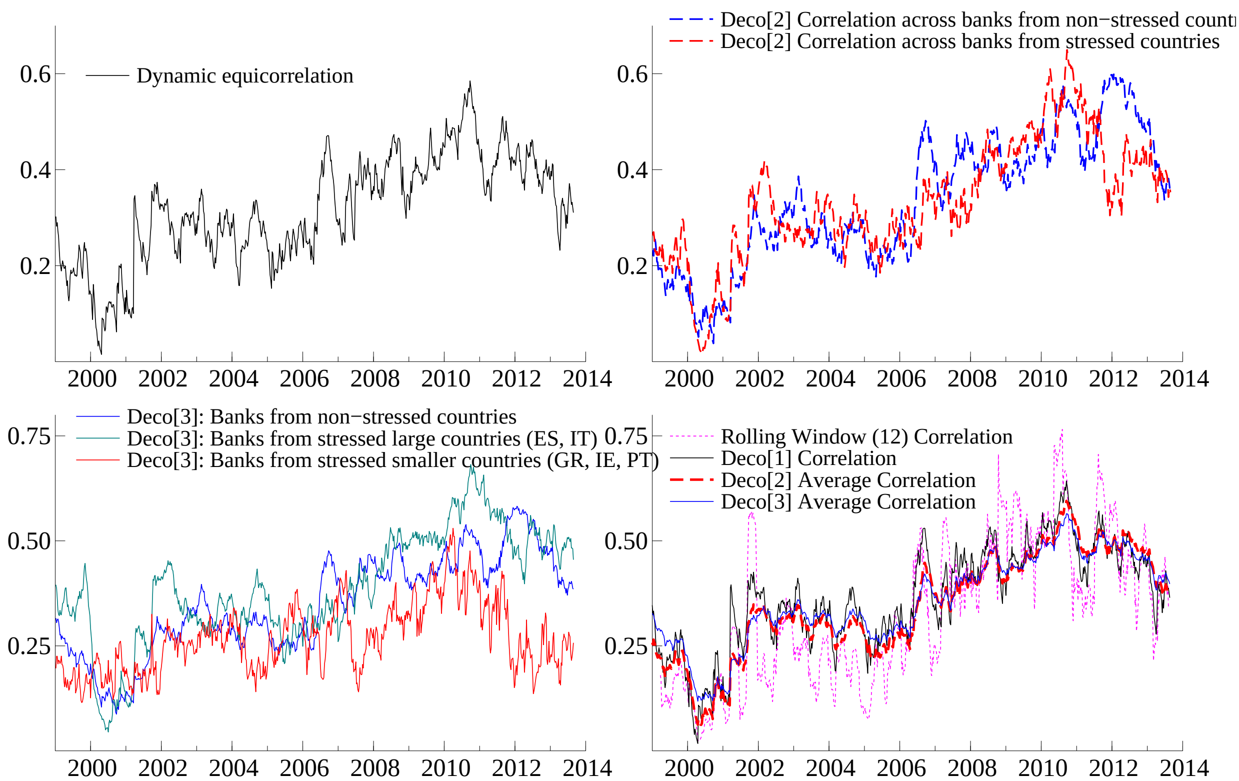

Figure 3: Filtered correlation estimates for all $N = 73$ financial firms

The panels plot dynamic equicorrelation estimates from different GHST block DECO models. We distinguish three block structures: 1 block (top left), 2 blocks (top right) and 3 blocks (bottom left). The bottom right panel benchmarks the equicorrelation estimates to the average correlation taken across $73(73-1)/2 = 2628$ pairwise correlation estimates based on a 12 weeks (approximately 3 moths) rolling window.

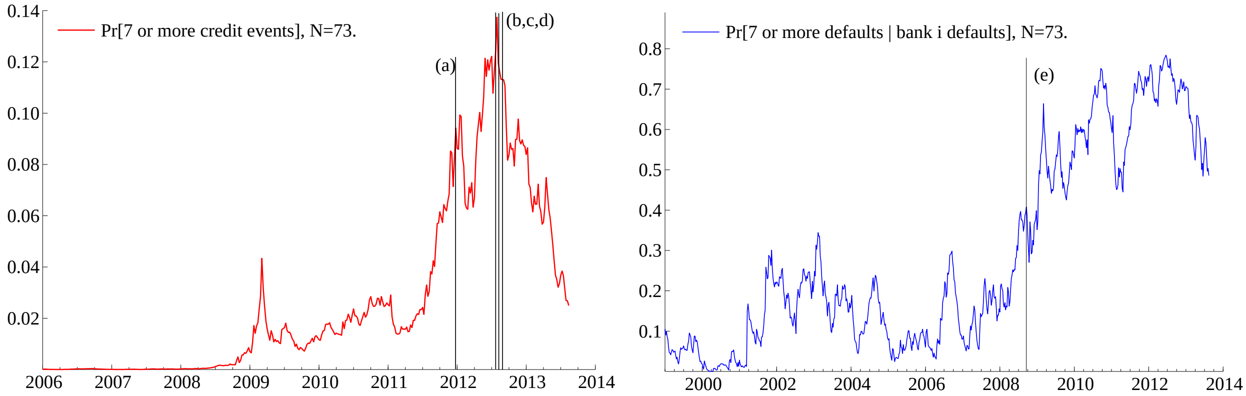

Figure 4: Joint and average conditional tail risk measures.

The left panel plots the joint tail risk measure (JRM) based on the GHST dynamic equicorrelation model. The JRM is the probability that 7 or more financial sector firms ($\bar{c} = 7/73 \approx 10\%$) experience a credit event over a 12 months ahead horizon, at any time t. The right panel plots the average conditional risk measure (CRM). The CRM is the average (over all 73 financial firms) conditional probability that $\bar{c} = 7/73 \approx 10\%$ or more financial firms experience a credit event given a credit event for a given firm i. All computations rely on the conditional law of large numbers (cLLN) approximation for the GHST DECO model.
The vertical lines in the left panel indicate the following events: (a) the allotment of the first (of two) 3y long term refinancing operations by the ECB on 21 December 2011, (b) a speech by the ECB president ("whatever it takes") on 26 July 2012, (c) the OMT announcement on 2 August 2012, and (d) the announcement of the OMT technical details on 6 September 2012. The vertical line in the right panel indicates the Lehman brothers bankruptcy on 15 September 2008.

tion 3. For the joint risk measure (JRM), we consider the probability that $\bar{c} = 7/73 \approx 10\%$ or more of currently active financial institutions experience a credit event over the next 12 months. The probability of such widespread and massive failure should typically be very small during non-crisis times. We plot the result in the left panel in Figure 4. As the JRM moves relatively little before 2008, we only plot it over the period 2006–2013. The JRM moves sharply upwards after the bankruptcy of Lehman Brothers in September 2008. The tail probability then remains approximately constant until the onset of the sovereign debt crisis in early 2010. It reaches a first peak in late 2011, followed by a second peak mid-2012.

The vertical lines in the left panel of Figure 4 indicate a number of relevant policy announcements. In late 2011, the announcement and implementation of two 3-year Long Term Refinancing Operations (3y-LTROs, allotted in December 2011 and February 2012) had a visible but temporary impact on financial sector tail risk.[5] In particular, the allotment of the first 3y-LTRO in late December 2011 appears to have lowered financial sector joint tail

[5] See ECB (2011) for the official press release and monetary policy objectives.

risk, temporarily, for a few months. In the first half of 2012, financial sector joint tail risk picks up again and rises to unprecedented levels until July 2012. The three vertical lines from July to September 2012 and the time variation in our joint risk measure strongly suggest that three events — a speech by the ECB president in London to do '*whatever it takes*' to save the euro on 26 July 2012, the announcement of the Outright Monetary Transactions (OMT) program on 2 August 2012, and the disclosure of the OMT details on 6 September 2012 — collectively ended this acute phase of extreme financial sector joint tail risks in the euro area. The joint risk measure decreases sharply, all the way until the end of the sample. The OMT is a program of the ECB under which the bank makes purchases ("outright transactions") in secondary sovereign bond markets, under certain conditions, of bonds issued by euro area member states. We refer to ECB (2012b) and Coeuré (2013) for the details on the OMT program. No purchases have yet been undertaken by the ECB within the OMT.

The right-hand panel in Figure 4 presents the average (across institutions) conditional risk measure for the 73 firms in our sample. At the start of the sample, there is little evidence of systemic clustering on average with low levels of the CRM between 0%–25%. The conditional probability rises substantially after the onset of the financial crisis. It peaks after the Lehman Brothers failure at levels of approximately 60%, with even higher peaks of approximately 80% during parts of the sovereign debt crisis. Such high levels of conditional tail probabilities signal strong interconnectedness among euro area financial institutions. One should also bear in mind, however, that the CRM is somewhat biased upwards due to the cLLN approximation. As can be seen in equation (26), the conditional probability given a default of firm i only considers the common risk variables κ_t and ς_t, and washes out all idiosyncratic risks $\tilde{\epsilon}_{jt}$ for $j \neq i$. At high levels of correlations, a default of firm i automatically implies that $\rho_t \kappa_t$ is very low given that y_{it} is below the default threshold y^*_{it}. As a result, given the low value of κ_t, subsequent defaults are much more likely because in the cLLN limiting approximation they cannot be off-set by idiosyncratic risks. We already saw, however, in the sample with $N = 10$ firms that the CRM limiting approximation still provides a good fit to the overall dynamic pattern of joint risk evolution in the sample. We therefore also take the current plot of the CRM as revealing the conditional risk dynamics over the sample period.

Interestingly, we find that the conditional risk measure is still quite high towards the end of the sample, despite the collapse in joint risk as shown in the left panel. The OMT announcements apparently have not brought down markets' perceptions of conditional (or contagion) risks in the euro area financial system as a whole to a comparable extent. Taken together, these findings suggests that the OMT may have been perceived by market participants as less of a 'firewall' measure that mitigates risk spillovers, but rather as a policy geared towards decreasing marginal risks but not necessarily systemic connectedness. Finally, our empirical results suggest that non-standard monetary policy measures (such as the 3y-LTROs and the OMT announcements) and financial stability tail risk outcomes are strongly related. This suggests substantial scope for the coordination of monetary, macro-prudential, and bank supervision policies. This is relevant as both monetary policy as well as prudential policies and banking supervision will be carried out jointly within the ECB as of November 2014.

5 Conclusion

We developed a novel and reliable modeling framework for estimating joint and conditional tail risk measures over time in a financial system that consists of many financial sector firms. For this purpose, we used a copula approach based on the generalized hyperbolic skewed Student's t (GHST) distribution, endowed with score driven dynamics of the generalized autoregressive score (GAS) type. Parsimony and flexibility were traded off by using a dynamic block-equicorrelation structure (block DECO). Using this structure, we were able to implement efficient approximations based on a conditional law of large numbers to compute joint and conditional tail probabilities of multiple defaults for a large set of firms. An application to euro area financial firms from 1999 to 2013 revealed unprecedented joint default risks during 2011-12. We also document the collapse of these joint default risks (but not conditional risks) after a sequence of announcements pertaining to the ECB's Outright Monetary Transactions program in August and September 2012.

References

Aas, K. and I. Haff (2006). The generalized hyperbolic skew student's t distribution. *Journal of Financial Econometrics 4*(2), 275–309.

Acharya, V., R. Engle, and M. Richardson (2012). Capital shortfall: A new approach to ranking and regulating systemic risks. *American Economic Review 102(3)*, 59–64.

Adrian, T., D. Covitz, and N. J. Liang (2013). Financial stability monitoring. *Fed Staff Reports 601*, 347–370.

Andres, P. (2014). Computation of maximum likelihood estimates for score driven models for positive valued observations. *Computational Statistics and Data Analysis*, forthcoming.

Avesani, R. G., A. G. Pascual, and J. Li (2006). A new risk indicator and stress testing tool: A multifactor nth-to-default cds basket. *IMF working paper, WP/06/105*.

Azzalini, A. and A. Capitanio (2003). Distributions generated by perturbation of symmetry with emphasis on a multivariate skew t distribution. *Journal of the Royal Statistical Society B 65*, 367–389.

Bauwens, L. and S. Laurent (2005). A new class of multivariate skew densities, with application to generalized autoregressive conditional heteroskedasticity models. *Journal of Business and Economic Statistics 23*(3), 346–354.

Bibby, B. and M. Sørensen (2001). Simplified estimating functions for diffusion models with a high-dimensional parameter. *Scandinavian Journal of Statistics 28*(1), 99–112.

Bibby, B. and M. Sørensen (2003). Hyperbolic processes in finance. In *Handbook of heavy tailed distributions in finance*, pp. 211–248. Elsevier Science Amsterdam.

Black, L. K., R. Correa, X. Huang, and H. Zhou (2012). The Systemic Risk of European Banks During the Financial and Sovereign Debt Crises. *Mimeo*.

Blasques, F., S. J. Koopman, and A. Lucas (2012). Stationarity and ergodicity of univariate generalized autoregressive score processes. *Tinbergen Institute Discussion Paper 12-059*.

Blasques, F., S. J. Koopman, and A. Lucas (2014a). Feedback effects, contraction conditions and asymptotic properties of the maximum likelihood estimator for observation-driven models. *Tinbergen Institute Discussion Paper*.

Blasques, F., S. J. Koopman, and A. Lucas (2014b). Information theoretic optimality of observation driven time series models. *Tinbergen Institute Discussion Paper 14-046*.

Blasques, F., S. J. Koopman, and A. Lucas (2014c). Maximum likelihood estimation for generalized autoregressive score models. *Tinbergen Institute Discussion Paper 14-029*.

Branco, M. and D. Dey (2001). A general class of multivariate skew-elliptical distributions. *Journal of Multivariate Analysis 79*, 99–113.

Christoffersen, P., K. Jacobs, X. Jin, and H. Langlois (2013). Dynamic dependence in corporate credit. *Mimeo*.

Coeuré, B. (2013). Outright Monetary Transactions, one year on. *Speech at the conference "The ECB and its OMT programme, Berlin, 02 September 2013, available at http://www.ecb.int*.

Creal, D., S. Koopman, and A. Lucas (2011). A dynamic multivariate heavy-tailed model for time-varying volatilities and correlations. *Journal of Business & Economic Statistics 29*(4), 552–563.

Creal, D., S. Koopman, and A. Lucas (2013). Generalized autoregressive score models with applications. *Journal of Applied Econometrics 28*(5), 777–795.

Creal, D., B. Schwaab, S. J. Koopman, and A. Lucas (2014). An observation driven mixed measurement dynamic factor model with application to credit risk. *The Review of Economics and Statistics, forthcoming* .

Demarta, S. and A. J. McNeil (2005). The t copula and related copulas. *International Statistical Review 73(1)*, 111–129.

Duffie, D., L. Saita, and K. Wang (2007). Multi-Period Corporate Default Prediction with Stochastic Covariates. *Journal of Financial Economics 83(3)*, 635–665.

ECB (2011). Ecb announces measures to support bank lending and money market activity. ECB press release, December 8.

ECB (2012a). European Central Bank Financial Integration Report 2012.

ECB (2012b). Technical features of Outright Monetary Transactions. ECB press release, September 6.

ECB (2014). The determinants of euro area sovereign bond yield spreads during the crisis. ECB Monthly Bulletin May 2014.

Engle, R. (2002). Dynamic conditional correlation. *Journal of Business and Economic Statistics 20*(3), 339–350.

Engle, R. and B. Kelly (2012). Dynamic equicorrelation. *Journal of Business & Economic Statistics 30*(2), 212–228.

Eser, F., M. Carmona Amaro, S. Iacobelli, and M. Rubens (2012). The use of the Eurosystem's monetary policy instruments and operational framework since 2009. ECB Occasional Paper 135, European Central Bank.

Eser, F. and B. Schwaab (2013). Assessing asset purchases within the ECBs Securities Markets Programme. *ECB Working Paper* (1587).

Giesecke, K., K. Spiliopoulos, R. B. Sowers, and J. A. Sirignano (2014). Large portfolio loss from default. *Mathematical Finance, forthcoming*.

Gordy, M. (2000). A comparative anatomy of credit risk models. *Journal of Banking and Finance 24*, 119–149.

Gordy, M. B. (2003). A risk-factor model foundation for ratings-based bank capital rules . *Journal of Financial Intermediation 12(3)*, 199–232.

Gupta, A. (2003). Multivariate skew-t distribution. *Statistics 37*(4), 359–363.

Hansen, B. E. (1994). Autoregressive conditional density estimation. *International Economic Review*, 705–730.

Hartmann, P., S. Straetmans, and C. de Vries (2004). Asset market linkages in crisis periods. *Review of Economics and Statistics 86(1)*, 313–326.

Hartmann, P., S. Straetmans, and C. de Vries (2007). Banking system stability: A cross-atlantic perspective. In M. Carey and R. M. Stulz (Eds.), *The Risks of Financial Institutions*, pp. 1–61. NBER and University of Chicago Press.

Harvey, A. and A. Luati (2014). Filtering with heavy tails. *Journal of the American Statistical Association, forthcoming*.

Harvey, A. C. (2013). *Dynamic Models for Volatility and Heavy Tails*. Cambridge University Press.

Harville, D. (2008). *Matrix algebra from a statistician's perspective*. Springer Verlag.

Hu, W. (2005). *Calibration of multivariate generalized hyperbolic distributions using the EM algorithm, with applications in risk management, portfolio optimization and portfolio credit risk.* Ph. D. thesis, Erasmus University Rotterdam.

Hull, J. and A. White (2004). Valuation of a CDO and an nth-to-default CDS without Monte Carlo simulation. *Journal of Derivatives 12*(2).

Hurvich, C. M. and C.-L. Tsai (1989). Regression and time series model selection in small samples. *Biometrika 76*, 297307.

Koopman, S. J., A. Lucas, and B. Schwaab (2011). Modeling frailty correlated defaults using many macroeconomic covariates. *Journal of Econometrics 162 (2)*, 312–325.

Koopman, S. J., A. Lucas, and B. Schwaab (2012). Dynamic factor models with macro, frailty, and industry effects for u.s. default counts: the credit crisis of 2008. *Journal of Business and Economic Statistics 30(4)*, 521–532.

Lucas, A., P. Klaassen, P. Spreij, and S. Straetmans (2001). An analytic approach to credit risk of large corporate bond and loan portfolios. *Journal of Banking & Finance 25*(9), 1635–1664.

Lucas, A., P. Klaassen, P. Spreij, and S. Straetmans (2003). Tail behaviour of credit loss distributions for general latent factor models. *Applied Mathematical Finance 10*(4), 337–357.

Lucas, A., B. Schwaab, and X. Zhang (2014). Conditional euro area sovereign default risk. *Journal of Business and Economic Statistics 32 (2)*, 271–284.

Lucas, A. and E. Silde (2014). Likelihood based dynamic equicorrelation. *Tinbergen Institute Discussion Paper*.

Malz, A. (2012). Risk-Neutral Systemic Risk Indicators. *FRB of New York Staff Report No. 607*.

Mencía, J. and E. Sentana (2005). Estimation and testing of dynamic models with generalized hyperbolic innovations. *CEPR Discussion Paper No. 5177*.

Oh, D. H. and A. Patton (2013). Time-varying systemic risk: Evidence from a dynamic copula model of cds spreads. *Working paper*.

Segoviano, M. A. and C. Goodhart (2009). Banking stability measures. *IMF Working Paper*.

Suh, S. (2012). Measuring systemic risk: A factor-augmented correlated default approach. *Journal of Financial Intermediation 21(2)*, 341–358.

Vasicek, O. (1987). Probability of loss on loan portfolio. *Working paper, Moody's Analytics Corporation.*

Zhang, X., D. Creal, S. Koopman, and A. Lucas (2011). Modeling dynamic volatilities and correlations under skewness and fat tails. *Tinbergen Institute Discussion Paper*.

Appendix A: technical details

Appendix A.1: Univariate volatility models

For full details and discussions on the univariate marginal modeling strategy used in this paper, we refer to Lucas et al. (2014). A short summary is as follows. Using the univariate GHST density

$$\begin{aligned}
p(y_t;\tilde{\sigma}_t^2,\gamma,\nu) &= \frac{\nu^{\frac{\nu}{2}}2^{1-\frac{\nu+1}{2}}}{\Gamma(\frac{\nu}{2})\pi^{\frac{1}{2}}\tilde{\sigma}_t}\cdot\frac{K_{\frac{\nu+1}{2}}\left(\sqrt{d(y_t)(\gamma^2)}\right)e^{\gamma(y_t-\tilde{\mu}_t)/\tilde{\sigma}_t}}{d(y_t)^{\frac{\nu+1}{4}}\cdot(\gamma^2)^{-\frac{\nu+1}{4}}},\\
d(y_t) &= \nu+(y_t-\tilde{\mu}_t)^2/\tilde{\sigma}_t^2,\\
\tilde{\mu}_t &= -\frac{\nu}{\nu-2}\tilde{\sigma}_t\gamma,\quad \tilde{\sigma}_t=\sigma_t T,\\
T &= \left(\frac{\nu}{\nu-2}+\frac{2\nu^2\gamma^2}{(\nu-2)^2(\nu-4)}\right)^{-1/2},
\end{aligned}$$

with $\sigma_t=\sigma(f_t)$ and $\sigma(f_t)=f_t^{1/2}$ or alternatively $\sigma(f_t)=\exp(f_t/2)$, the score driven dynamics allowing for a leverage effect are given by

$$\begin{aligned}
f_{t+1} &= \tilde{\omega}+\sum_{i=0}^{p-1}A_i s_{t-i}+\sum_{j=0}^{q-1}B_j f_{t-j}+C(s_t-s_t^{\mu})1\{y_t<\mu_t\},\\
s_t &= \mathcal{S}_t\nabla_t,\quad \nabla_t=\partial\ln p(y_t|\mathcal{F}_{t-1};f_t,\theta)/\partial f_t,\\
s_t^{\mu} &= \mathcal{S}_t\nabla_t^{\mu},\quad \nabla_t^{\mu}=\partial\ln p(\mu_t|\mathcal{F}_{t-1};f_t,\theta)/\partial f_t,\\
\nabla_t &= \Psi_t H_t\left(w_t\cdot y_t^2-\tilde{\sigma}_t^2-\left(1-\frac{\nu}{\nu-2}w_t\right)\tilde{\sigma}_t\gamma y_t\right),\\
w_t &= \frac{\nu+1}{2d(y_t)}-\frac{k'_{0.5(\nu+1)}\left(\sqrt{d(y_t)\cdot(\gamma^2)}\right)}{\sqrt{d(y_t)/(\gamma^2)}},\\
\Psi_t &= \frac{\partial\sigma_t}{\partial f_t},\quad H_t=T\tilde{\sigma}^{-3}.
\end{aligned}$$

Using this univariate model, we obtain the univariate filtered volatilities for N=10 financial firms as discussed in Section 4.2. We do not report the volatility plots for space considerations.

Appendix A.2: The dynamic GHST score

This subsection proves Result 1.

Proof. Let $k_\lambda(\cdot) = \ln K_\lambda(\cdot)$ with first derivative $k'_\lambda(\cdot)$. We use the following matrix calculus results for an invertible matrix X, and column vectors α and β:

$$\frac{\partial(\alpha' X^{-1}\beta)}{\partial \text{vec}(X)} = -((X')^{-1} \otimes X^{-1})\text{vec}(\alpha\beta'), \quad \frac{\partial(\log|X|)}{\partial \text{vec}(X)} = ((X')^{-1} \otimes X^{-1})\text{vec}(X).$$

Based on these results one obtains

$$\begin{aligned}
\nabla_t &= \frac{\partial \text{vec}(\tilde{\Sigma}_t)'}{\partial f_t} \frac{\partial \ln p(y_t; \tilde{\Sigma}_t, \gamma, \nu)}{\partial \text{vec}(\tilde{\Sigma}_t)} \\
&= \Psi'_t \left(-w_t \frac{\partial d(y_t)}{\partial \text{vec}(\tilde{\Sigma}_t)} + \check{w}_t \frac{\partial d(\gamma)}{\partial \text{vec}(\tilde{\Sigma}_t)} + \frac{\partial(\gamma' \tilde{\Sigma}_t^{-1}(y_t - \tilde{\mu}))}{\partial \text{vec}(\tilde{\Sigma}_t)} - \frac{1}{2} \frac{\partial(\log(|\tilde{\Sigma}_t|))}{\partial \text{vec}(\tilde{\Sigma}_t)} \right) \\
&= \Psi'_t H_t \text{vec}\left(w_t (y_t - \tilde{\mu})(y_t - \tilde{\mu})' - \check{w}_t \gamma\gamma' - \gamma(y_t - \tilde{\mu})' - 0.5\tilde{\Sigma}_t \right),
\end{aligned}$$

with $H_t = \tilde{\Sigma}_t^{-1} \otimes \tilde{\Sigma}_t^{-1}$, and

$$w_t = \frac{\nu + N}{4d(y_t)} - \frac{k'_{0.5(\nu+N)}\left(\sqrt{d(y_t)d(\gamma)}\right)}{2\sqrt{d(y_t)/d(\gamma)}}, \quad \check{w}_t = \frac{\nu + N}{4d(\gamma)} + \frac{k'_{0.5(\nu+N)}\left(\sqrt{d(y_t)d(\gamma)}\right)}{2\sqrt{d(\gamma)/d(y_t)}}.$$

□

Appendix A.3: The GHST m-block DECO model

Assume that N firms can be divided up into m different groups, and that firms have equicorrelation ρ_i^2 within each group, $i = 1, \ldots, m$, $\rho_i \cdot \rho_j$ between groups i and j, $j = i+1, \ldots, m$. There are n_i firms in group i. The block-equicorrelation model proposed here differs from Engle and Kelly (2012) in that there is a direct relation between the equicorrelation in the off-diagonal blocks and the diagonal blocks. We impose this restriction to maintain the factor copula structure in Section 2.1 that permits the quick computations of the joint and conditional risk measures discussed in Section 3.

In the dynamic GHST m- block equicorrelation case the scale matrix at time t is given by

$$\tilde{\Sigma}_t = \begin{pmatrix} (1-\rho_{1,t}^2)\mathrm{I}_1 & \ldots & \ldots & 0 \\ 0 & (1-\rho_{2,t}^2)\mathrm{I}_2 & \ldots & 0 \\ \vdots & \vdots & \ddots & \vdots \\ 0 & 0 & \ldots & (1-\rho_{m,t}^2)\mathrm{I}_m \end{pmatrix} + \begin{pmatrix} \rho_{1,t}\ell_1 \\ \rho_{2,t}\ell_2 \\ \vdots \\ \rho_{m,t}\ell_m \end{pmatrix} \cdot \begin{pmatrix} \rho_{1,t}\ell_1 \\ \rho_{2,t}\ell_2 \\ \vdots \\ \rho_{m,t}\ell_m \end{pmatrix}', \tag{A1}$$

where I_i is an $n_i \times n_i$ identity matrix, $\ell_i \in \mathbb{R}^{n_i \times 1}$ is a column vector of ones, and $|\rho_{it}| < 1$. The block structure of the matrix allows us to obtain analytical solutions for the determinant,

$$\det(\tilde{\Sigma}_t) = \left[1 + \frac{n_1\rho_{1,t}^2}{1-\rho_{1,t}^2} + \cdots + \frac{n_m\rho_{m,t}^2}{1-\rho_{m,t}^2}\right](1-\rho_{1,t}^2)^{n_1} \cdots (1-\rho_{m,t}^2)^{n_m}, \tag{A2}$$

see Harville (2008). This matrix determinant result further facilitates the computation of the likelihood and the score steps in high dimensions. The GAS updating equations are as follows.

Result 4. *Assume that y_t follows a GHST distribution and that its time-varying scale matrix $\tilde{\Sigma}_t$ has a block equicorrelation structure which contains $m \times m$ blocks as in* (A1). *Factor f_t is an $m \times 1$ vector such that $\rho_i = (1 + \exp(-f_{it}))^{-1}$ for $i = 1, 2, \cdots, m$. For the system* (9)–(12),

$$
\begin{aligned}
\tilde{\Psi}_t &= \frac{\partial \mathrm{vec}(\tilde{\Sigma}_t)'}{\partial f_t} = \frac{\partial \mathrm{vec}(\tilde{\Sigma}_t)'}{\partial \rho_t} \frac{d\rho_t'}{df_t}, \\
\frac{d\rho_t'}{df_t} &= \begin{bmatrix} \frac{\exp(-f_{1,t})}{(1+\exp(-f_{1,t}))^2} & 0 & \cdots & 0 \\ 0 & \frac{\exp(-f_{2,t})}{(1+\exp(-f_{2,t}))^2} & \cdots & 0 \\ \vdots & \vdots & \ddots & \vdots \\ 0 & 0 & \cdots & \frac{\exp(-f_{m,t})}{(1+\exp(-f_{m,t}))^2} \end{bmatrix}, \\
\frac{\partial \mathrm{vec}(\tilde{\Sigma}_t)}{\partial \rho_t{}'} &= \left[\mathrm{vec}\begin{pmatrix} \mathrm{I}_1 & \cdots & 0 \\ \vdots & \ddots & \vdots \\ 0 & \cdots & 0 \end{pmatrix}, \cdots, \mathrm{vec}\begin{pmatrix} 0 & \cdots & 0 \\ \vdots & \ddots & \vdots \\ 0 & \cdots & \mathrm{I}_m \end{pmatrix} \right] \cdot \begin{pmatrix} -2\rho_{1,t} & 0 & \cdots & 0 \\ \vdots & \vdots & \ddots & \vdots \\ 0 & 0 & \cdots & -2\rho_{2,t} \end{pmatrix} \\
&+ \left[\begin{pmatrix} \rho_{1,t}\ell_1 \\ \rho_{2,t}\ell_2 \\ \vdots \\ \rho_{m,t}\ell_m \end{pmatrix} \otimes \mathrm{I}_N + \mathrm{I}_N \otimes \begin{pmatrix} \rho_{1,t}\ell_1 \\ \rho_{2,t}\ell_2 \\ \vdots \\ \rho_{m,t}\ell_m \end{pmatrix} \right] \cdot \left[\begin{pmatrix} \ell_1 \\ 0 \\ \vdots \\ 0 \end{pmatrix}, \cdots, \begin{pmatrix} 0 \\ 0 \\ \vdots \\ \ell_{n_m} \end{pmatrix} \right].
\end{aligned}
$$

Proof. Using results from differential calculus, the result follows from the fact that

$$
\frac{\partial \mathrm{vec}(\tilde{\Sigma}_t)'}{\partial \rho_{it}} = -2\rho_{it} \cdot \mathrm{vec}\begin{bmatrix} 0 & 0 & \cdots & 0 \\ \vdots & \vdots & \ddots & \vdots \\ 0 & 0 & \mathrm{I}_i & 0 \\ 0 & 0 & \cdots & 0 \end{bmatrix} + \left[\begin{pmatrix} \rho_{1,t}\ell_1 \\ \rho_{2,t}\ell_2 \\ \vdots \\ \rho_{m,t}\ell_m \end{pmatrix} \otimes \mathrm{I}_N + \mathrm{I}_N \otimes \begin{pmatrix} \rho_{1,t}\ell_1 \\ \rho_{2,t}\ell_2 \\ \vdots \\ \rho_{m,t}\ell_m \end{pmatrix} \right] \cdot \begin{pmatrix} 0 \\ \vdots \\ \ell_{n_i} \\ 0 \end{pmatrix},
$$

and by combining this expression across the m groups. □